Radiological dispersal device outdoor simulation test: Cesium chloride particle characteristics

Sang Don Lee [a,*], Emily G. Snyder [a], Robert Willis [a], Robert Fischer [c], Dianne Gates-Anderson [c], Mark Sutton [c], Brian Viani [d], John Drake [b], John MacKinney [e]

[a] U.S. Environmental Protection Agency, Research Triangle Park, NC 27711, United States
[b] U.S. Environmental Protection Agency, Cincinnati, OH 45268, United States
[c] Lawrence Livermore National Laboratory, Livermore, CA 94550, United States
[d] Simbol Mining Corp., Pleasanton, CA 94566, United States
[e] U.S. Department of Homeland Security, Washington, DC 20528, United States

ABSTRACT

Particles were generated from the detonation of simulated radiological dispersal devices (RDDs) using non-radioactive CsCl powder and explosive C4. The physical and chemical properties of the resulting particles were characterized. Two RDD simulation tests were conducted at Lawrence Livermore National Laboratory: one of the simulated RDDs was positioned 1 m above a steel plate and the other was partially buried in soil. Particles were collected with filters at a distance of 150 m from the origin of the RDD device, and particle mass concentrations were monitored to identify the particle plume intensity using real time particle samplers. Particles collected on filters were analyzed via computer-controlled scanning electron microscopy coupled with energy dispersive X-ray spectrometry (CCSEM/EDX) to determine their size distribution, morphology, and chemical constituents. This analysis showed that particles generated by the detonation of explosives can be associated with other materials (e.g., soil) that are in close proximity to the RDD device and that the morphology and chemical makeup of the particles change depending on the interactions of the RDD device with the surrounding materials.

Published by Elsevier B.V.

1. Introduction

A radiological dispersal device (RDD) is any device that spreads radioactive material in the environment with malicious intent. The archetypal RDD, also called a dirty bomb, is the combination of a conventional explosive device with radioactive materials that can be obtained from industrial, commercial, medical and research applications [1,2]. An RDD attack can impact a society in various ways including creation of casualties, disruption of the economy, and potentially desertion of the contaminated area [3–5]. Highly populated urban areas would likely be the primary target for an RDD attack to maximize the impact. Development of fast and cost-effective decontamination technologies is essential to minimize the social and economic damage. In order to facilitate the development of RDD specific decontamination procedures or to better deploy existing radionuclide decontamination methods in the event of an RDD, detailed information describing the chemical and physical characteristics of explosively generated radioactive particles is needed.

Harper et al. [6] have studied RDD material aerosolization and Gates-Anderson et al. [7] investigated particle deposition on concrete surfaces using simulated RDDs. The study by Harper et al. [6] concluded that aerosolization potential and particle size and morphology characteristics from an RDD explosion are mainly dependent on the RDD material type and device geometry. However, it is necessary to investigate the impact of near-field properties on particle characteristics and also obtain more experimental data which can be used to develop and validate predictive models for the dispersal of radioactive particles subsequent to an RDD event.

The focus of this study was to characterize explosively generated particle properties at a set distance from the explosion site by evaluating the impact of surrounding materials on the formation and subsequent composition and deposition of RDD particles. These simulated RDD tests were conducted under a collaborative effort between the U.S. Environmental Protection Agency (EPA) and Lawrence Livermore National Laboratory (LLNL). The simulated RDDs were prepared with non-radioactive cesium chloride (CsCl) and C4 high explosive. This paper discusses the effect of the

* Corresponding author at: U.S. Environmental Protection Agency, 109 T.W. Alexander Dr., MD E343-06, Research Triangle Park, NC 27711, United States. Tel.: +1 919 541 4531; fax: +1 919 541 0496.
E-mail address: lee.sangdon@epa.gov (S.D. Lee).

near-field on particle properties and the particle characteristics resulting from these simulated RDDs.

2. Experimental

2.1. Test Description

The explosive RDD simulation tests were carried out at the Department of Energy's Lawrence Livermore National Laboratory Site 300 facility. The building 851 (B-851) firing facility was used to support these tests. Two RDD simulation tests were conducted: Test I was designed to explosively aerosolize technical grade CsCl powder (average powder size of 190 μm, Shelton Scientific, Poesta, IA) in an RDD suspended 1 m above a steel plate which prevented ground soil aerosolization during explosion. Test II was designed to explosively aerosolize CsCl powder in an RDD partially buried in soil. Wind speed and direction were monitored every second and saved as 15 min averages using a permanent tower weather station (Met One 010C and 020C, Met One Instruments, Inc., Grants Pass, OR). Relative humidity (HMP45A, Vaisala, Inc., Boston, MA) and temperature (Met One 60A, Met One Instruments, Inc., Grants Pass, OR) data were also collected.

2.2. Sampling and Measurement

A total of three sampling stations were positioned in an arc 150 m from the explosion location for Tests I and II. Each sampling station included open-faced polycarbonate filter (37 mm, 0.4 μm pore, SKC, Eighty Four, PA) samplers for particle size and morphology analysis, open-faced Teflon filter (37 mm, 0.45 μm pore size, SKC, Eighty Four, PA) samplers for cumulative cesium mass quantification and real time particle monitors (SIDEPAKs, AM510, TSI, Minneapolis, MN) for real time particle mass measurement. Each sampling station was positioned 12 m apart from the other sampling stations. All particle samplers were placed approximately 70 cm above the ground. Sampling locations were selected 30 min before each detonation in accordance with the wind direction.

Filter samples were collected at a flow rate of 2.0 L min^{-1} using portable industrial hygiene pumps (Aircheck 2000, SKC, Eighty Four, PA). The pump flow rates were calibrated using a Dry Cal (Defender 500 Series, Bios International, Butler, NJ) calibrator. Two blank filters were collocated at the selected sampling locations. Filter samplers were started 30 min before the explosion and they were stopped after the site was ensured to be safe for reentrance. The sampling duration after explosion was at least 1 h. Each filter was visibly examined before loading it onto the sampling cassette and damaged filters were discarded. After sampling, filters were taken out of their sampling cassettes and secured in Petri dishes that were placed in an airtight container for transportation to the analysis laboratory. Two collocated field blanks (one polycarbonate filter and one Teflon filter, with no airflow through the filters) were collected at one sampling location for each of the two tests.

Three SIDEPAK sampling stations were also positioned at the 150 m arc sampling locations. SIDEPAKs measure the mass concentration of particles larger than 0.1 μm and have adjustable inlets which dictate the size range of particles that are measured via a laser photometer. Each sampling station had two SIDEPAKs with PM$_{2.5}$ (particles are 2.5 μm in diameter and smaller) and PM$_{10}$ (particles are 10 μm in diameter and smaller) inlets. Sampling lines for each of the SIDEPAKs were identical in length and type. Particle mass concentration was monitored for a total of 2 h: 1 h before and 1 h after the explosion. During the monitoring period, SIDEPAKs were operated with the flow rate of 1.7 L min^{-1}, and particle mass concentration data were recorded every second. Flow rates of all

Table 1
Experimental conditions for Tests I and II.

Conditions	Test I	Test II
Date	April 23, 2007	April 24, 2007
Detonation time	12:26 pm (PDT)	11:25 am (PDT)
RDD Material	CsCl (2 kg)	CsCl (2 kg)
Explosive	C-4 (2.2 kg)	C-4 (2.2 kg)
Device location	1 m above a large steel plate placed on the ground	Entrapped ~5 cm in the soil
Wind direction	347°	309°
Wind speed	7 m s^{-1}	2 m s^{-1}
Temperature	17 °C	22 °C
Relative humidity	42%	25%
Sampling locations at 150 m arc	310°, 330°, 350°	230°, 250°, 270°

SIDEPAKs were checked before and after each operation using the Dry Cal calibrator.

2.3. Analysis of Cesium Containing Particle

Cesium containing particle characteristics were determined by computer-controlled scanning electron microscopy (CCSEM) coupled with energy dispersive X-ray spectrometry (EDX). CCSEM/EDX analyses were conducted in the Electron Microscopy Laboratory of the U.S. EPA's National Exposure Research Laboratory. A Personal SEM^{TM} (PSEM, R.J. Lee Group, Inc., Instruments Division, Trafford, PA) was used for the analyses. Polycarbonate filters were transported to the laboratory and mounted on 25 mm aluminum stubs using double-sided carbon tape. The mounted filters were coated with ~150 Å of carbon using a carbon coating system (model 108A, Cressington Scientific Instruments, UK) to reduce sample surface charging. The CCSEM/EDX analyses included the identification of Cs particles, determination of particle shape and morphology, average diameter (0.4–100 μm), elemental composition, and identification of the individual particle locations on the substrate. A particle was designated as a Cs containing particle (Cs particle) if at least 5% of its total EDX signal could be attributed to Cs. This Cs particle rule was set by manual analyses of multiple Cs particles before computer-controlled operation and the criteria were set where the EDX signal count of Cs is low enough to detect all Cs containing particles and higher than background spectral signals. Large particles were probed manually before computer-controlled operation and no particles larger than 100 μm were detected. The CCSEM/EDX was operated in the backscattered electron (BE) mode optimized to identify Cs particles and was operated at 500× magnification, zero degrees tilt, 16 mm working distance, and 20 kV accelerating voltage. Higher resolution micrographs of Cs particles were obtained using a LEO 440 SEM (Carl Zeiss SMT, Inc., Peabody, MA) integrated with IMIX EDX system (Princeton Gamma Tech, Inc., Princeton, NJ).

The cesium mass on the Teflon filters was determined via inductively coupled plasma/mass spectrometry (ICP/MS) according to EPA Method 6020 [8]. Teflon filters were transported to the laboratory and cesium ions were extracted by sonication in a dilute nitric acid solution (less than 2% by volume in deionized water).

3. Results and discussion

Experimental conditions for two RDD tests are summarized in Table 1. Meteorological information is provided at 12:30 pm (April 23, 2007) and 11:30 am (April 24, 2007) for Tests I and II, respectively. The simulated RDDs were prepared with equal amounts of cesium chloride powder and C4; the most significant difference between the two tests was the position of two simulated RDDs. The simulated RDD in Test I was positioned one meter above a steel plate (2.54 m × 2.54 m × 0.025 m) which was laid on the ground to

prevent soil entrainment during CsCl aerosolization. During Test II, the device was partially buried in a round plastic basin (1.5 m diameter, 0.5 m deep) filled with 0.57 m^3 of compacted soil. The plastic basin was placed on the steel plate used in Test I. The relative humidity levels during both tests were below the CsCl particle deliquescent point, 68% RH, which suggests that all CsCl particles were dispersed as solid particles [9,10]. Initially, there was a concern that there could be Cs particle contamination due to resuspension of Test I particles from activities at the site, but no Cs particles were found on filter samples taken prior to Test II detonation.

3.1. Real time particle concentration

Total particle mass concentrations, for particles larger than 0.1 μm, were monitored with SIDEPAKs over the course of both tests. Time series particle mass concentrations at three different locations are shown in Figs. 1 and 2 for Tests I and II, respectively. Data shown in Figs 1 and 2 were extracted from the full data set to show the rise in particle mass signal after the detonation. According to the SIDEPAK data before detonation, the average background particle concentration was less than 10 μg m^{-3} for both test days. As seen in Fig. 1, SIDEPAKs at the location points 330° and 350° in Test I showed strong particle signal about 20 s after the detonation which lasted for approximately 1 min. The SIDEPAK monitors at the location 310° did not show any significant particle mass change. Data for the SIDEPAKs with two different aerodynamic particle size cutoffs (2.5 and 10 μm) are also shown in Figs. 1 and 2. Data for the SIDEPAKs equipped with the different inlets in Test I showed a similar pattern and intensity, which implies that particles collected from this explosion are mostly smaller than 2.5 μm.

SIDEPAK data from Test II in Fig. 2 demonstrate that a continuous particle plume similar to that shown by Test I data was not observed. Time series data in Fig. 2 show several separated peaks after detonation. SIDEPAKs measure all types of particles and Cs particles cannot be distinguished from the overall particle plume. Cs particles were further identified and characterized in the polycarbonate filter samples that were collected next to the SIDEPAKs.

3.2. Particle characteristics

Particles collected on polycarbonate filters from Tests I and II were analyzed by CCSEM/EDX. The total analyzed surface areas of individual filters ranged between 0.12 and 1.50 cm^2, depending generally on particle loading. Particles were categorized into two different groups: Cs particles and other particles. The filter analysis results from Test I are summarized in Table 2. Particle concentrations were normalized to 1 cm^2 of filter area assuming uniform particle deposition on the filters. The raw numbers of particles detected, before normalization, are shown in parentheses to provide an indication of counting statistics. Because duplicate samples were not collected at each site, it was not possible to determine the precisions of the particle concentrations shown in Table 2. We estimate concentration uncertainties of 20%, based on other CCSEM-based field studies. The results showed that the total number of particles per unit area is higher for the samplers at the locations of 350° and 330° but there is an insignificant concentration of particles at the sampler located at 310°. This result is consistent with the SIDEPAK data. In addition, the majority of particles collected at the 350° location are Cs particles, and this result was confirmed by ICP/MS analysis of Teflon filters at this station
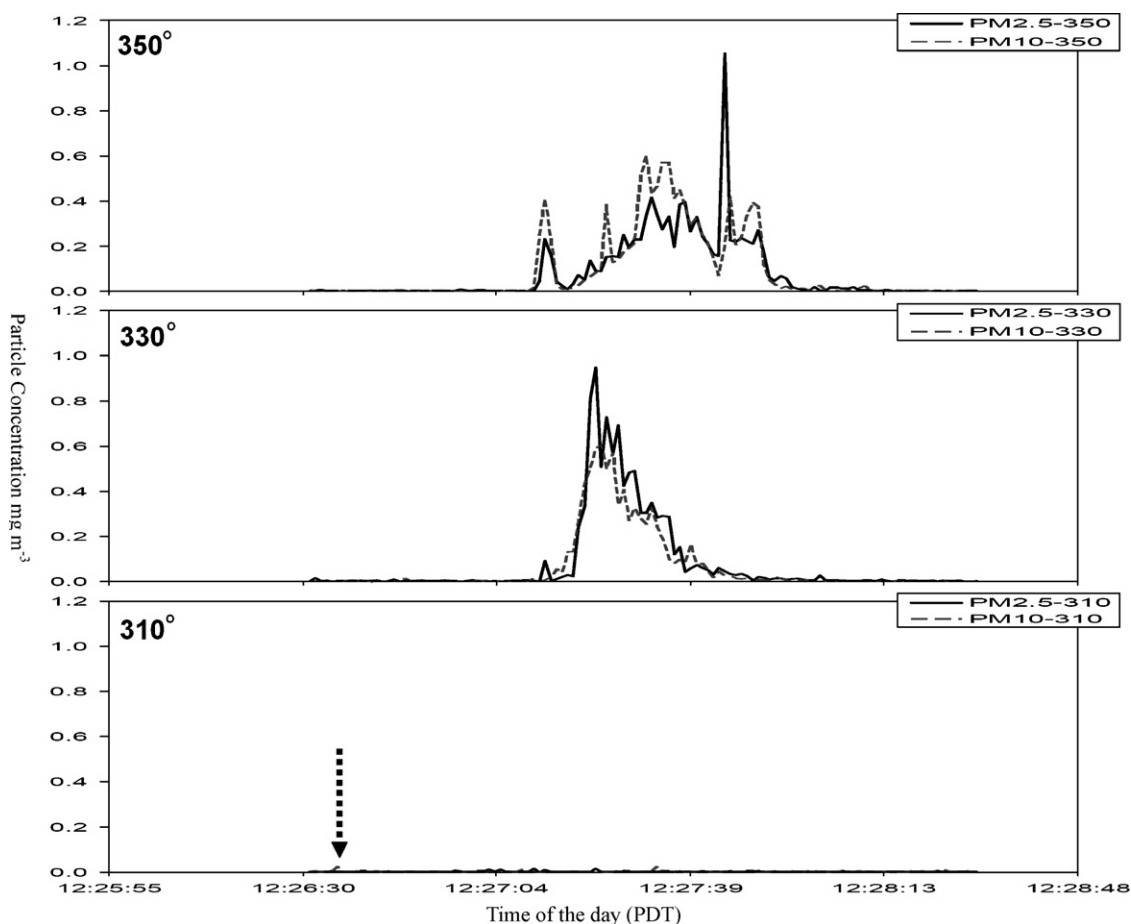

Fig. 1. Time series particle mass concentration measured using SIDEPAKs for Test I on April 23rd (detonation time is marked with a dotted arrow).
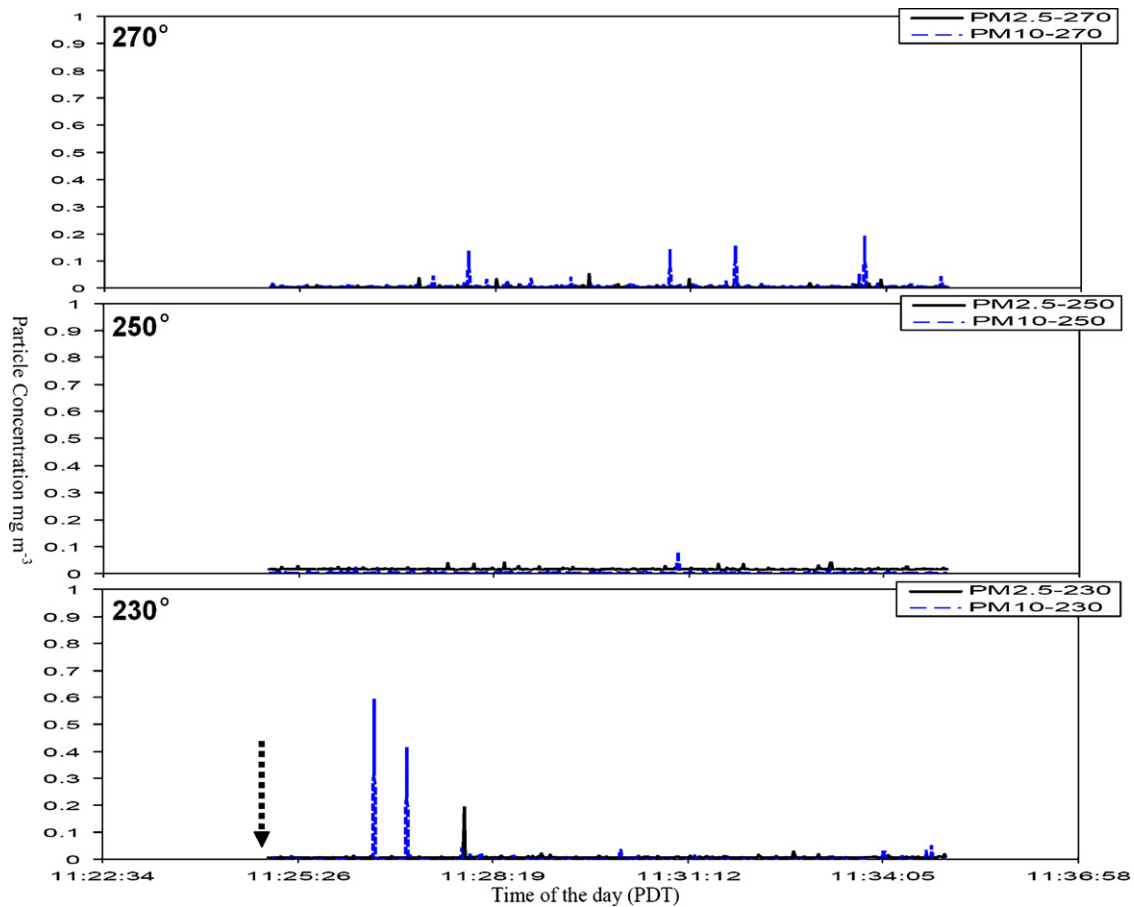
Fig. 2. Time series particle mass concentration measured using SIDEPAKs for Test II on April 24th (detonation time is marked with a dotted arrow.).

(Table 2). Polycarbonate filter analysis results from Test II show that a total number of Cs particles was less than 1% of total analyzed particles from Test II and this is also consistent with ICP/MS analysis, where the Cs concentration on all three filters was below the method detection limit.

Geometric mean diameters of Cs particles from Tests I and II, estimated by CCSEM/EDX analyses, were 0.93 and 1.14 μm with geometric standard deviation of 1.79 and 1.92, respectively. CCSEM/EDX size analysis is based on the particle's physical projected area (not aerodynamic diameter). CCSEM/EDX uses the contrast difference between the particles and the polycarbonate

Table 2
Summary of Particle Analysis.

Sampling location	SEM/EDX (cm^{-2})[a]		ICP/MS (μg)
	Cs particles	Other particles	Cs mass
Test I			
310°	0	440 (405)	n.d.[b]
330°	6,703 (3237)[a]	5,776 (2790)	0.89
350°	22,107 (2683)	2,612 (317)	1.39
Field blank			
350°	0	737 (430)	n.d.
Test II			
230°	0	2,155 (1322)	n.d.
250°	0	1,839 (1425)	n.d.
270°	84 (126)	12,608 (18917)	n.d.
Field blank			
230°	0	433 (255)	n.d.

[a] Numbers in parentheses are raw, un-normalized particle counts.
[b] n.d. stands for 'not detected'.

substrate to identify and size particles in the BE mode. Because the BE mode has difficulty differentiating carbonaceous features from the polycarbonate filter substrate, some Cs particles attached to carbonaceous particles (from the detonation of C4) may be counted as separate particles while carbonaceous features may be biased by underestimating particle sizes and missing altogether. Therefore, the actual particle size in the atmosphere may differ from the value estimated by CCSEM/EDX.

Cs particles from the Test I 350° sampling station were imaged using the LEO S440 SEM, and these images are shown in Fig. 3. Most of the particles collected at the 150 m sampling stations were smaller than 10 μm, as shown in Fig. 3(a) and (b), and a small portion of particles (less than 1% in number) were as large as 10 μm as shown in (c) and (d). The small and large particles in Fig. 3 show different morphologies. Particles (a) and (b) in Fig. 3 appear to be agglomerations of multiple micron-sized particles while larger particles in (c) and (d) show the irregular shape of particles deposited onto the surface. These differences in size and morphology of Cs particles suggest that particles may be generated by different mechanisms such as phase transitions for small particles such as those shown in Fig. 3(a) and (b) and mechanical processes for large particles such as those shown in Fig. 3(c) and (d).

The large particles (c) and (d) in Fig. 3 are imaged in both the secondary electron (SE) mode (left half) and the BE mode (right half). The BE signal increases monotonically with atomic number so that BE images can reveal compositional differences within a single particle (features with higher atomic number appear brighter) [11]. Secondary electrons are emitted from the surface of a feature; thus, the SE image is more sensitive to a particle's surface morphology [11]. Comparison of images from the two modes can provide complementary information for the selected particle as to
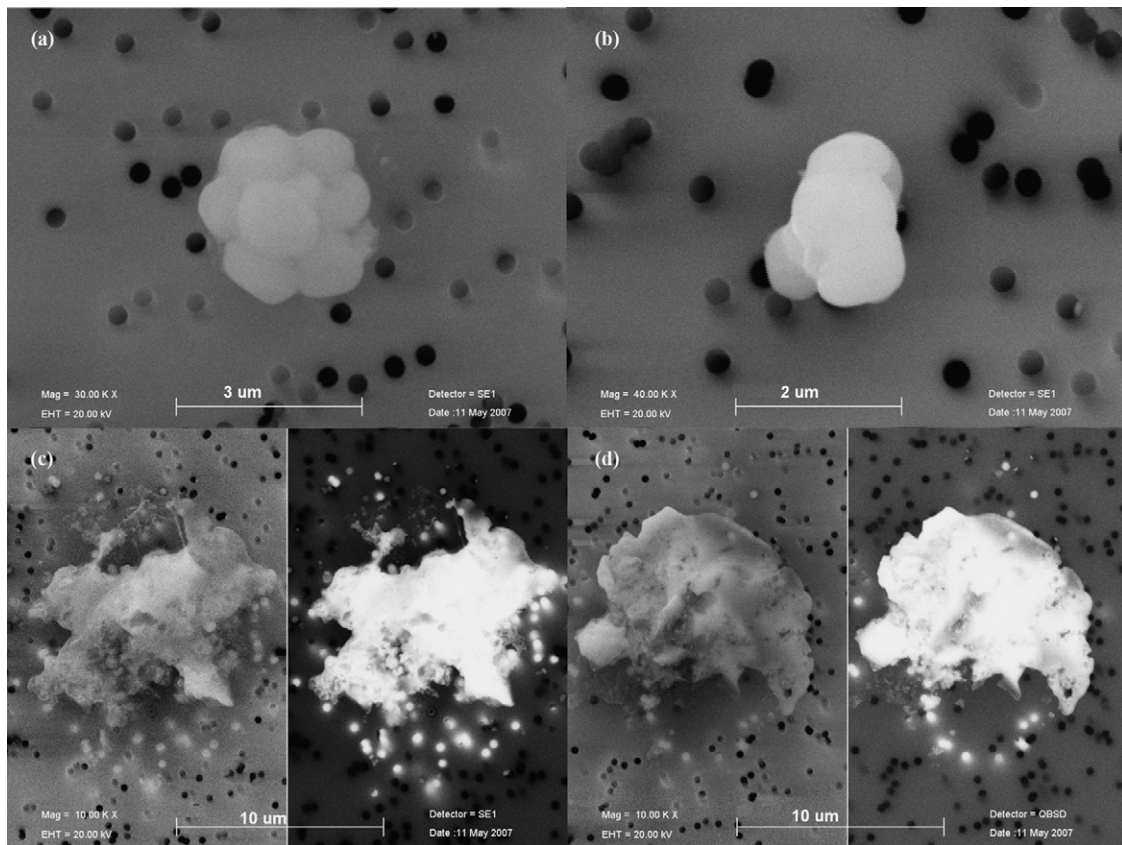
Fig. 3. LEO 440 SEM micrographs of Cs particles from Test I. Black circular dots approximately 0.5 μm in diameter are pores of polycarbonate collection filters. Figures (c) and (d) show side-by-side images in SE mode (left half) and BE mode (right half). Particle picture of SE and BE modes show that single material (Cs) is major element of particles.
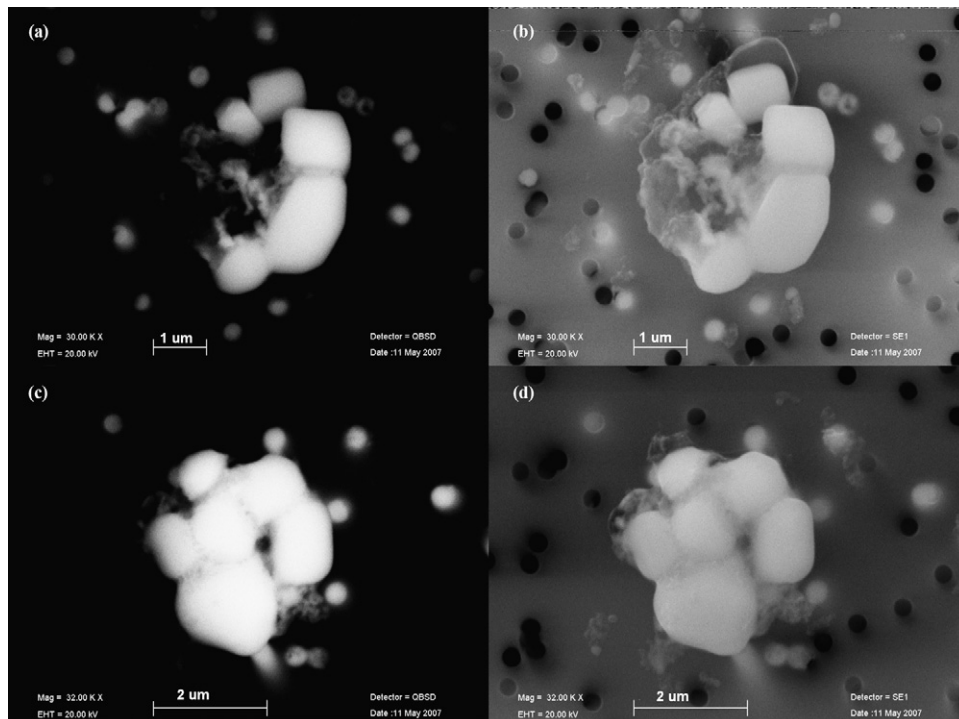

Fig. 4. Particle image (LEO 440 SEM) comparison using BE mode (a and c) and SE mode (b and d) for two particles from Test I. SE images (b and d) show presence of carbonaceous material connecting Cs particles.
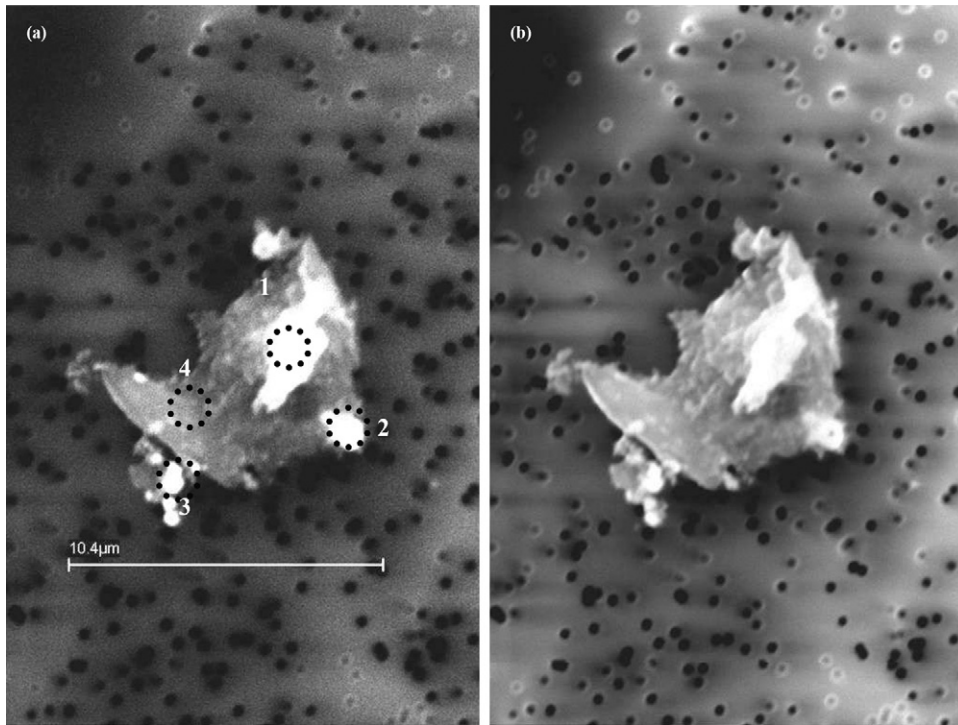
Fig. 5. BE image (LEO 440 SEM) of a large Test I particle show several Cs areas within a larger carbonaceous matrix. Circled areas in BE image (a) were further analyzed with EDX to identify major elements in this particle.
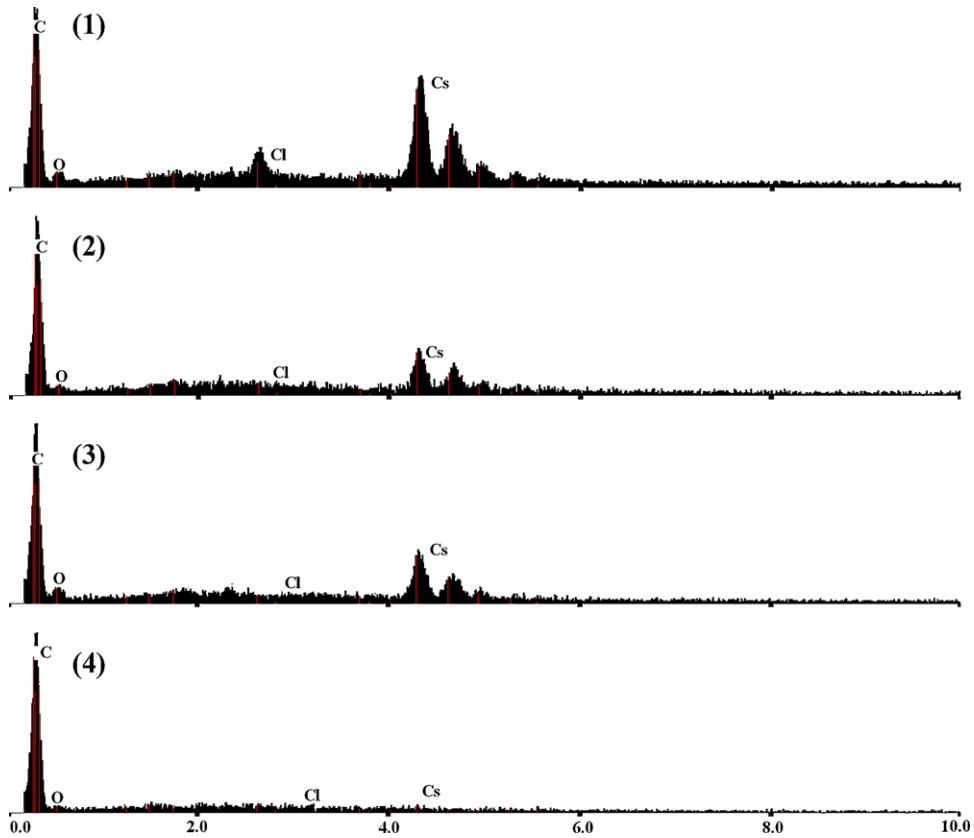

Fig. 6. EDX spectra collected within the circled areas shown in Test I particle from Fig. 5.
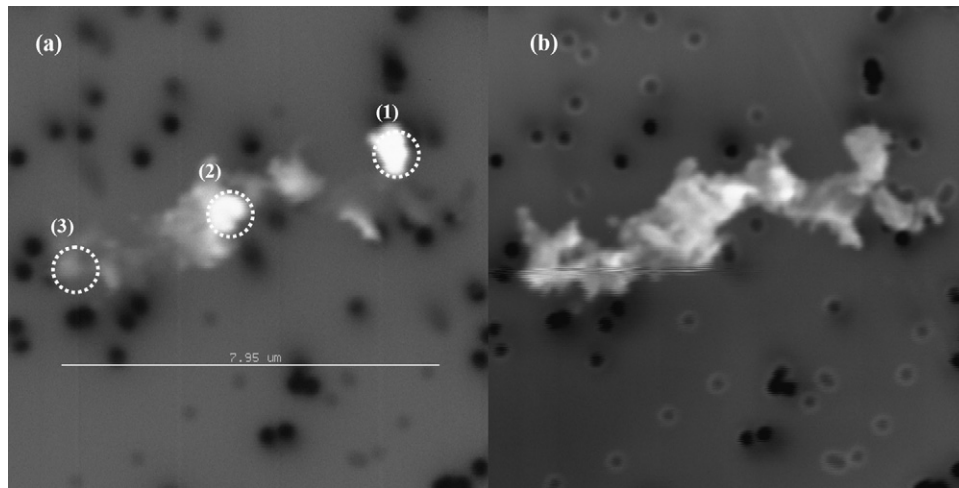
Fig. 7. BE (a) and SE (b) images of a Test II particle showing high Cs areas (1 and 2) within a larger carbonaceous feature. Images are prepared with PSEM.

how the Cs is associated with other elements in a particle. The particle shapes in Fig. 3(c) and (d) determined in the two modes (BE and SE) are similar, so these particles are mainly composed of one material, Cs. The images in Fig. 4 show that other materials are frequently associated with Cs particles. The SE images in Fig. 4(b) and (d) indicate the presence of a thin layer of low atomic number material (that is absent from the BE image in Fig. 4(a) and (c)) that appears to connect or envelop the relatively bright Cs particles. EDX analysis reveals that this material consists of mostly carbon and Fig. 4(c) and (d) shows similar features. An example of Cs containing large particles is shown in Fig. 5. The particle(s) shown in Fig. 5 appear(s) to be an agglomeration of carbonaceous material (darker region) and Cs particles (bright features). EDX spectra collected within the four different areas circled in the BE image are shown in Fig. 6. The bright areas (1, 2, and 3) show clear Cs peaks while the darker area 4 shows only carbon. These and other features indicate that many Cs particles are associated with carbonaceous material possibly derived from the C4 explo-

sive material. Another important aspect of the X-ray spectra shown in Fig. 6 is the chlorine content. Chlorine is observed in the spectrum collected from area 1 but not in areas 2 and 3. The EDX peak area ratios of chlorine to cesium show wide variation from 0 to 3 for the Cs particles analyzed from the 350° Test I station, and approximately 60% of all Cs particles show Cl/Cs ratios below 1. Although these ratios relate only qualitatively to the actual ratio of Cs to Cl atoms in the feature of interest, it is apparent that many CsCl particles lose their association with chlorine through an unknown mechanism.

The association of Cs particles with the surrounding soil material during an explosion was also observed in samples collected during Test II. The feature shown in Fig. 7(b) (SE mode) is an aggregate of chemically distinct particles, shown by the different levels of brightness in the BE image (Fig. 7(a)). The unseen material in Fig. 7(a) is carbonaceous, similar to the particles shown in Figs. 4(a) and (c). EDX analyses of the three areas circled in white in Fig. 7(a) are shown in Fig. 8. All three X-ray spectra show the elements C,
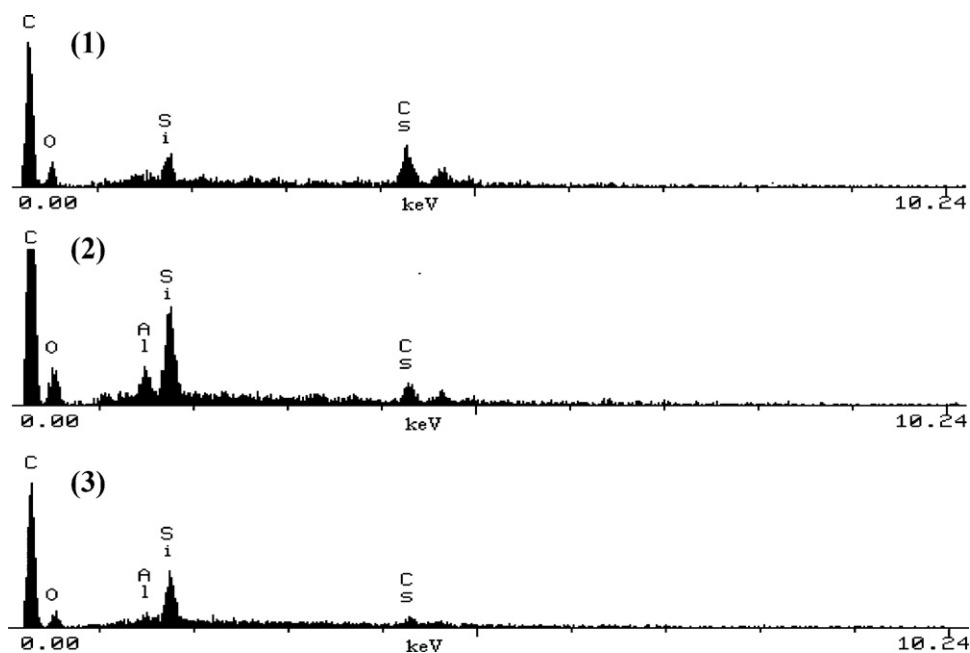

Fig. 8. EDX spectra collected within the circled areas (1–3) shown in Test II particle from Fig. 7.
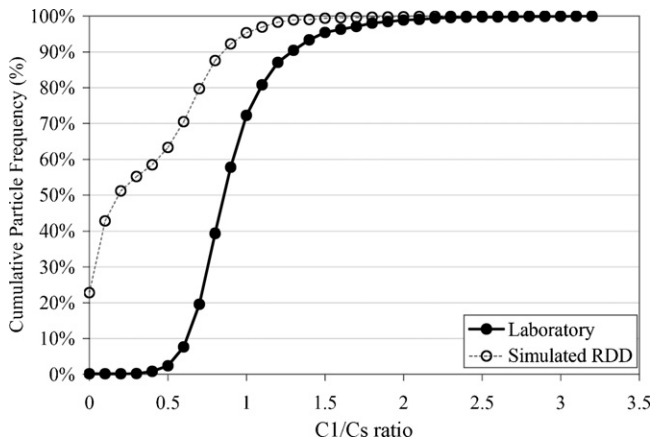
Fig. 9. Comparison of cumulative frequency distribution for Cl/Cs ratio in Cs particles generated in laboratory versus simulated RDD (Test I).

O, Al, Si, and Cs. The brightest area in Fig. 7(a) is associated with the highest Cs concentration, while the least bright area (circle 3) in Fig. 7(a) shows much less Cs and more Al and Si. The Al, Si and possibly some of the carbonaceous material observed in association with Cs particles may have originated from soil resuspended during the explosion, since Test II was conducted with the RDD partially buried in the soil. A total of 68 Cs particles were identified by CCSEM/EDX on the Test II filters, and more than 50 of these particles were manually analyzed. Approximately 80% of the analyzed Cs particles were associated with Si–Al rich material as well as carbonaceous material. While it is difficult to generalize conclusions based on the limited number of particles analyzed, most of the Cs particles containing carbonaceous material also contained aluminosilicate materials.

3.3. Chlorine Content in Cesium Particles

Cs containing particle CCSEM/EDX results from Test I showed insignificant amounts of Cl in Cs particles (Fig. 6) consistent with the results from Test II (Fig. 8). The low Cl counts in Cs particles were further investigated by comparing the ratios of Cl and Cs in particles from the field RDD tests to the Cs particles prepared in the laboratory. In the laboratory, Cs particles were prepared by aerosolizing a CsCl-methanol solution and collecting the aerosolized particles on a carbon coated glass substrate. After drying, the particles were analyzed by CCSEM/EDX using the simulated RDD particle analysis parameters. Over 4000 Cs particles were identified and the average Cl/Cs ratios were compared to those from Test I (2683 Cs particles). The average (standard deviation) of Cl/Cs ratio for the laboratory-generated Cs particles is 0.92 (0.31) versus 0.32 (0.37) for the simulated RDD Cs particles. The cumulative particle frequency distributions for Cl/Cs ratios are shown in Fig. 9. More than 60% of the Cs particles from Test I are lower than 5% (the Cl/Cs ratio is 0.73) of the cumulative particle frequency for the laboratory-generated Cs particles. This clearly shows that CsCl particles from the simulated RDDs were altered in the explosion process. Test II results were not included in this analysis due to the limited number of Cs particles observed during the analysis.

4. Conclusions

In this study, the physical and chemical characteristics of particles from two simulated CsCl RDD events were analyzed using SEM/EDX. Because of the limited nature of the study (i.e., Tests I and II could not be repeated in this study), one must be cautious in generalizing these results to actual RDD explosions. Comparison of the two different RDD scenarios showed the potential for aerosolized Cs particles to interact with the surrounding soil during the blast. Explosively generated Cs particles may be altered by agglomeration with other surrounding materials and these agglomerated Cs particles may disperse differently depending on the area around the RDD due to the increased particle mass of these particles. Further, low chlorine content, indicated by the higher Cl/Cs ratios of the laboratory-generated Cs particles, was observed in Cs particles from both tests. The change in the CsCl composition due to the explosion potentially affects Cs particles' post-deposition interactions and the subsequent efficacy of the RDD decontamination methods. Therefore, it is necessary to investigate the impact of this altered Cs particle composition in the framework of the fate and transport of Cs on surfaces. This information will help plan specific decontamination procedures and develop better decontamination methods.

References

[1] U.S. Nuclear Regulatory Commission, http://www.nrc.gov/reading-rm/doc-collections/fact-sheets/dirty-bombs-bg.html, 2007 (the last access on May 2009).
[2] A.J. Gonzalez, Security of radioactive sources: threats and answers, in: International Conference on Security of Radioactive Sources, International Atomic Energy Agency, Vienna, Austria, 2003, pp. 33–58.
[3] H. Rosoff, D. von Winterfeldt, A risk and economic analysis of dirty bomb attacks on the ports of Los Angeles and long beach, Risk Anal. 27 (2007) 533–546.
[4] P.A. Karam, Radiological terrorism, Hum. Ecol. Risk Assess. 11 (2005) 501–523.
[5] P.D. Zimmerman, C. Loeb, Dirty bombs: the threat revisited, Defense Horizons 38 (2004) 1–11.
[6] F.T. Harper, S.V. Musolino, W.B. Wente, Realistic radiological dispersal device hazard boundaries and ramifications for early consequence management decisions, Health Phys. 93 (2007) 1–16.
[7] D. Gates-Anderson, C. Rasmussen, R. Fischer, B. Viani, Q.H. Hu, M. Sutton, W. McNab, Dirty bomb fallout, Nucl. Eng. Int. 52 (2007) 28–29.
[8] U.S. Environmental Protection Agency, Method 6020, Inductively Coupled Plasma-Mass Spectrometry, EPA Office of Research and Development, 1994.
[9] M.E. Wise, G. Biskos, S.T. Martin, L.M. Russell, P.R. Buseck, Phase transitions of single salt particles studied using a transmission electron microscope with an environmental cell, Particul. Sci. Technol. 39 (2005) 849–856.
[10] S.T. Martin, Phase transitions of aqueous atmospheric particles, Chem. Rev. 100 (2000) 3403–3454.
[11] J. Goldstein, D.E. Newbury, D.C. Joy, C.E. Lyman, P. Echlin, E. Lifshin, L.C. Sawyer, J.R. Michael, Scanning Electron Microscopy and X-ray Microanalysis, 2nd ed., Kluwer Academic/Plenum, New York, 1992, pp. 92–93.